Supplementary information for: Marco Wende, Jule Grunewald, Ada Bachmann, Fabian Wilde, Michael Heymann, Alois M. Herkommer, Valese Aslani, and Andrea Toulouse. “Illumination and microscopy combined in a single fibre bundle by 3D-printed micro-optics”. Light: Advanced Manufacturing

Supplement 2

1. Contrast improvement by integrated illumination with the ring-DOE

We experimentally quantify the impact of our integrated illumination technique by a ring-DOE at the fiber front-end. Therefore, we compare the contrast with an imaging procedure that uses straight epi-illumination without the ring-DOE. For this case, we illuminate the CFB back-end through the same objective lens used for imaging. We perform the same image processing routine from Methods K on both images in Fig. S1. Without ring-DOE, the image contrast is low despite dark-subtraction; reliably recognizing the observed structures (group 6, elements 3-5 of a positive USAF 1951 Resolution Target, Edmund Optics, Barrington, New Jersey, USA) is not possible. In comparison, the ring-DOE has a perceivably better contrast, and the line-contrast (same scale for both lines) is ~ 2.5-fold higher.

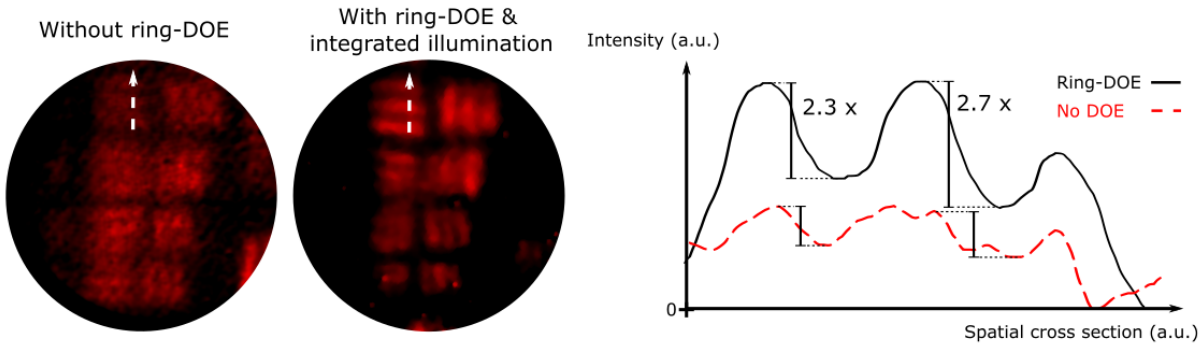

Fig. S1: Comparison of imaging contrast without- and with the ring-DOE for integrated illumination. For simultaneous imaging and illumination, the contrast of an off-the shelf CFB is inadequate. Using our new approach for integrated illumination by a ring-DOE, the contrast increases ~2.5-fold.

2. Effect of fiber bending on the imaging stability

The imaging robustness against endoscope-bending is a major challenge for many ultracompact endoscope architectures, but central for practical applicability. Hence, we study the effects of endoscope bending on our endoscope’s imaging stability in our experimental setup (Fig. S2 **a**).

Before approaching the sample, we turn on the integrated ring-illumination and acquire a single image for dark-subtraction. We then place the group 6, elements 3-5 of a USAF target (Positive USAF 1951 Resolution Target, Edmund Optics, Barrington, New Jersey, USA) in the endo-microscope’s field of view. Then we proceed with imaging, manually bending the fiber differently for each acquired image as illustrated in Fig. S2 **a**. The images were processed with the routine described in Methods K in the main manuscript. When bending the CFB, we observed that notable differences in the images mainly occur when considerable strain (Fig. S2 **b**) displaces the mounted CFB end-facets. At the CFB front-end, the movement relatively to the sample causes defocus; at the CFB back-end, the movement relatively to the back-end relay microscope causes a mismatch to the dark-image and decreases the quality of the dark-subtraction, visible in the second image in Fig. S2 **b.** The latter issue is addressable computationally by improved CFB-facet tracking and real-time alignment between the dark-image image and the fiber-bundle [1], or experimentally by more rigid fiber mounts.

We used a standard commercial CFB (FIGH-10-350S, Fujikura Ltd., Japan), and the observed stability likely transfers to comparable CFBs. Nevertheless, this must be experimentally confirmed when using other CFB-

models, because their different core-density, -size, -shape, and -variability could alter the inter-core crosstalk strength [3] – especially when combined with longer illumination wavelengths.

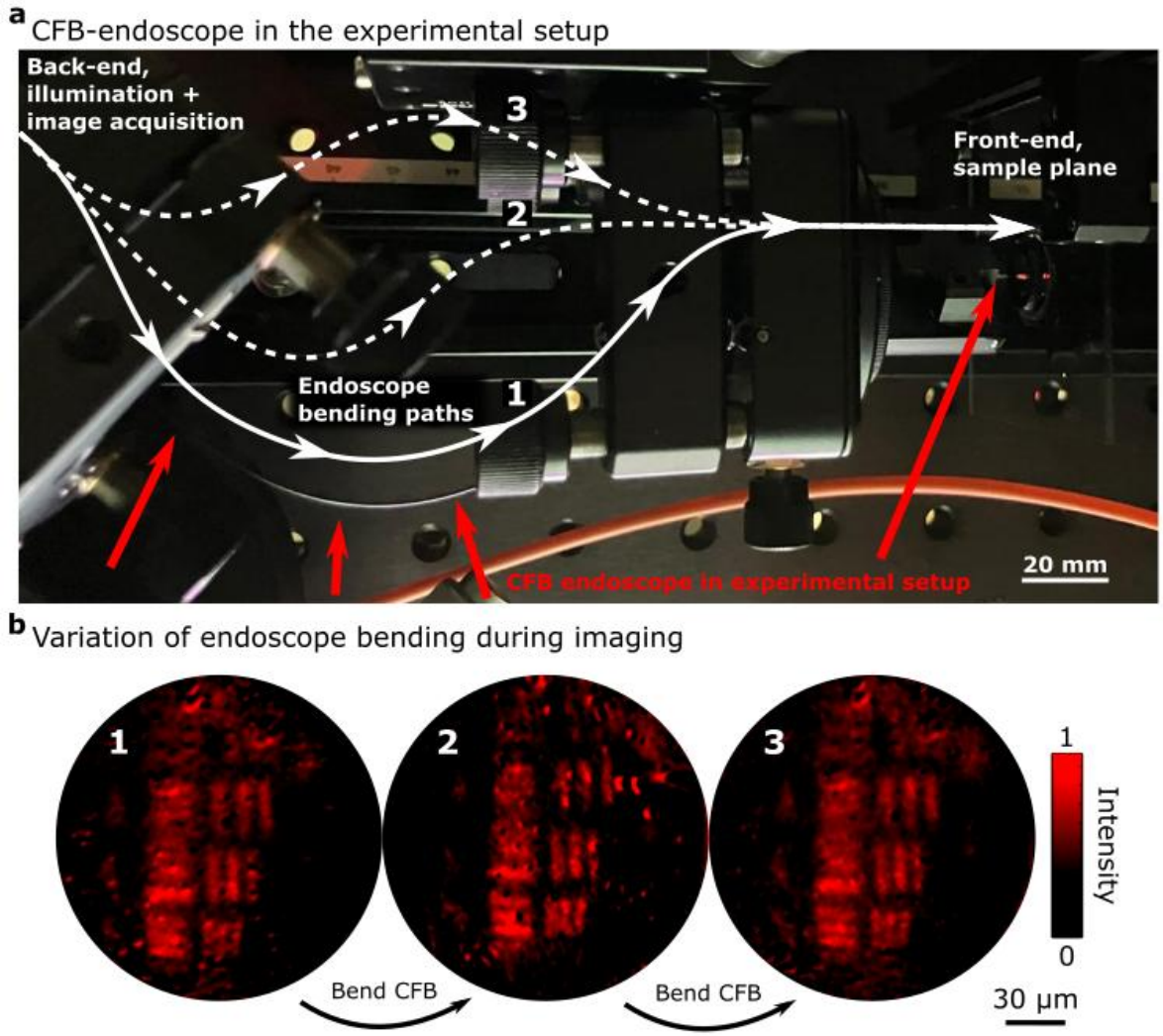

Fig. S2: Experimental CFB-endoscope imaging setup. **a** We perform illumination and image acquisition at the fiber back-end (left). The sample is placed at the endoscope’s front-end on the right. The red arrows indicate the CFB in the setup, and the white lines illustrate the CFB bending paths used for image acquisition. In this experiment, we manually bend the endoscope for each acquired image. **b** Imaging (in air, USAF group 6 elements 3-5) for the different CFB-bending paths. We observed differences mainly when strain displaced the CFB-facets in the mounts, causing a spatial mismatch in the dark-image subtraction.

Supplementary information for: Marco Wende, Jule Grunewald, Ada Bachmann, Fabian Wilde, Michael Heymann, Alois M. Herkommer, Valese Aslani, and Andrea Toulouse. “Illumination and microscopy combined in a single fibre bundle by 3D-printed micro-optics”. Light: Advanced Manufacturing

3. Imaging system resolution simulation

To theoretically investigate the contributions limiting the lateral imaging resolution, we perform a resolution cascade simulation of our endoscopic imaging system. We therefore use methods and MATLAB-code from Ref. 2, with our system parameters listed in Table S1. The MATLAB-program calculates the individual modulation transfer functions (MTFs) of the proximal relay-microscope, the coherent fiber bundle (CFB), and the distal endo-microscope. The individual MTFs are then multiplied (= cascaded) to obtain the system MTF.

Table S1: Parameters used in the resolution cascade simulation [2].

Proximal microscope magnification	**20 x**
Proximal microscope numerical aperture	**0.42**
Sensor pixel size	**4.8 µm**
CFB	**2 µm [3]**
CFB core spacing	**3.2 µm [3]**
Endo-microscope magnification for n = 1.0/n = 1.4	**0.98/1.35**
Endo-microscope numerical aperture for n = 1.0/n = 1.4	**0.4/0.55**

The CFB-pixelation is a likely bottleneck for the total system resolution. The hexagonal core-arrangement in the CFB (Fig. S3) further introduces a spatial dependence to the maximum sampling resolution. The simulation considers the spatial dependence using the two spatial frequency coordinates ξ and η, accounting for the expected upper and lower boundary of the resolution limit imposed by the CFB pixelation.

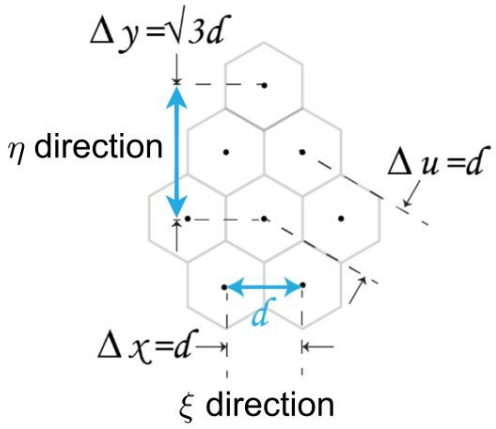

Fig. S3: CFB core arrangement as defined in the resolution cascade simulation. ξ and η are the corresponding spatial frequencies. Figure adapted from Ref. 2.

Supplementary information for: Marco Wende, Jule Grunewald, Ada Bachmann, Fabian Wilde, Michael Heymann, Alois M. Herkommer, Valese Aslani, and Andrea Toulouse. “Illumination and microscopy combined in a single fibre bundle by 3D-printed micro-optics”. Light: Advanced Manufacturing

Fig. S4 visualizes the simulated system MTF for our endoscope in air (**a**) and in immersion (**b**). The vertical lines indicate the theoretical resolution limits imposed by the CFB-pixelation (solid lines), and by the Rayleigh criterion (26.3 % residual contrast [4]). Table S2 summarizes the extracted resolution limits in frequency-space; Table S3 shows the corresponding distances in object-space.

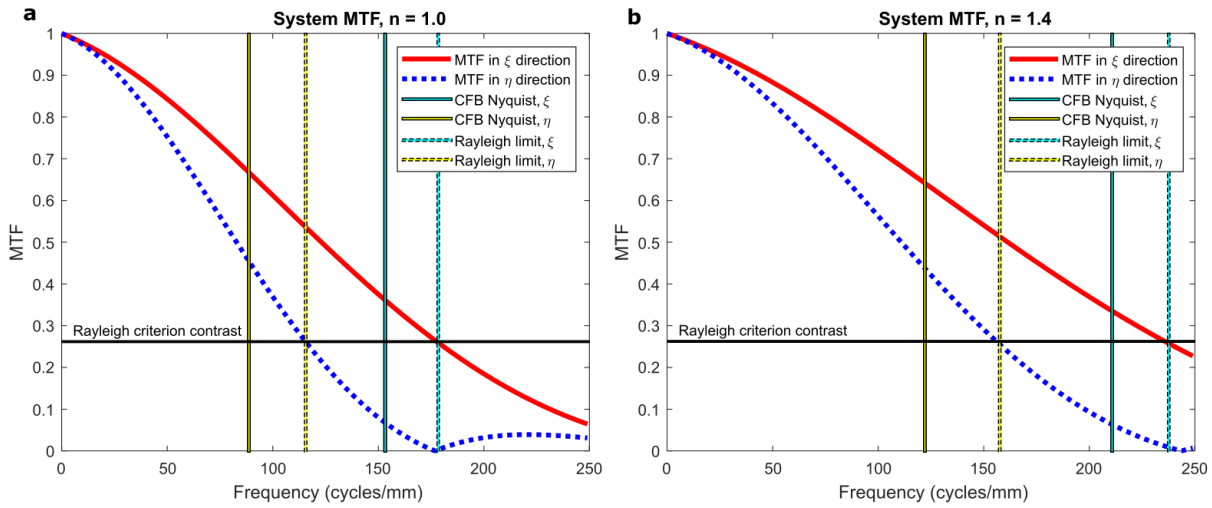

Fig S4: Simulated system modulation transfer functions. The vertical lines indicate object plane resolution limits for the spatial frequencies ξ and η, considering the Rayleigh-criterion (26.3 % contrast [4]) and the Nyquist frequency for the CFB-core sampling. The system MTF considers the cascaded MTF’s of the proximal imaging system (camera-pixelation + relay-microscope, the CFB-pixelation, and the distal 3D-printed endo-microscope. **a** MTF in air with n = 1.0. **b** MTF in immersion with n = 1.4.

We use the lower resolution boundary values (spatial/frequency coordinates $\Delta x/\xi$) for comparison with the experimental values in our main manuscript. As the inter-core spacing varies by ~ 10 % [3] for our CFBs (FIGH-10-350S, Fujikura Ltd., Japan), these simulated values offer useful approximations for the attainable resolution, but variations both upward and downward have been reported and are thus expected [2].

Table S2: Simulated resolvable spatial frequency in object-space

Refractive index	ξ, Nyquist (cycles/mm)	η, Nyquist (cycles/mm)	ξ, Rayleigh (cycles/mm)	η, Rayleigh (cycles/mm)
n = 1	153	89	177	115
n = 1.4	205	122	238	156

Table S3: Simulated spatial resolution in object-space

Refractive index	x, Nyquist (µm)	y, Nyquist (µm)	x, Rayleigh (µm)	y, Rayleigh (µm)
n = 1	6.5	11.2	5.6	8.7
n = 1.4	4.8	8.7	4.2	6.4

Supplementary information for: Marco Wende, Jule Grunewald, Ada Bachmann, Fabian Wilde, Michael Heymann, Alois M. Herkommer, Valese Aslani, and Andrea Toulouse. “Illumination and microscopy combined in a single fibre bundle by 3D-printed micro-optics”. Light: Advanced Manufacturing

4. Effect of filtering on acquired images

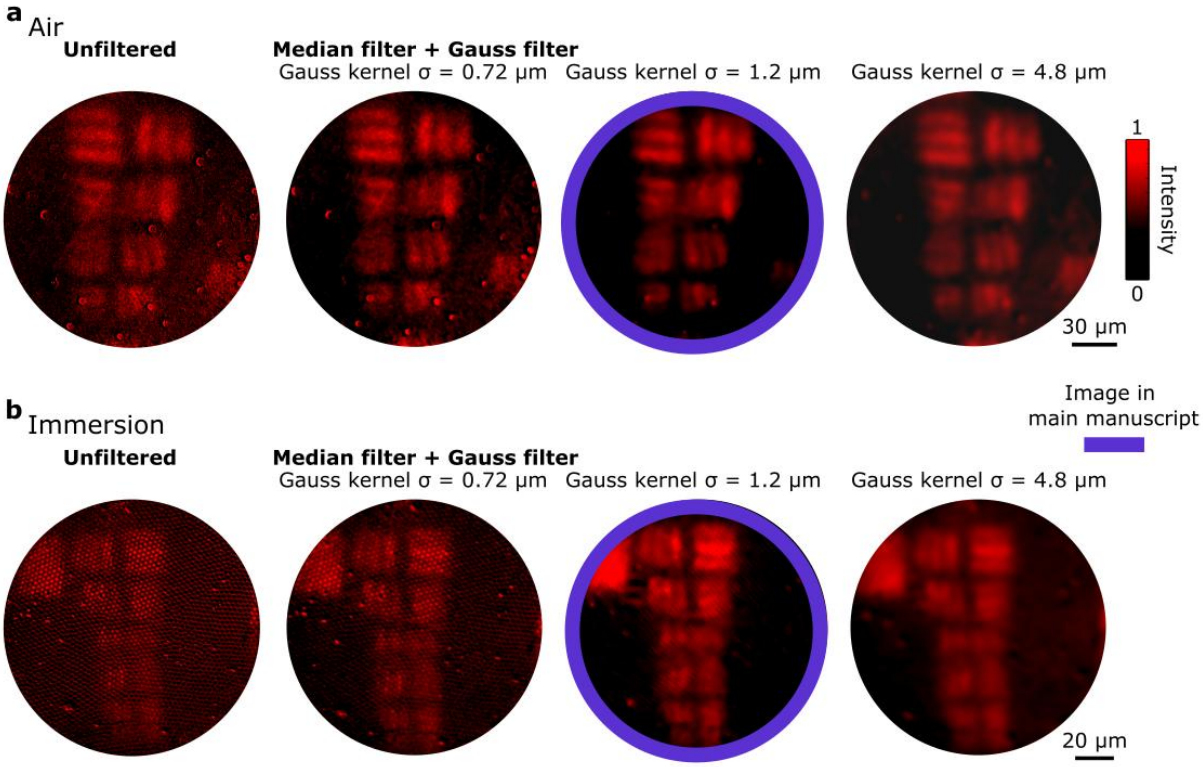

Fig. S5: Influence of filtering on image appearance of the resolution targets from Fig. 6. The leftmost column shows the images after dark-subtraction without further filtering. The applied standard deviation σ for the Gaussian kernel increases from the left to right. First, the CFB-pixelation artifacts are removed; then, the images increasingly blur without further benefit. **a** USAF target in air (n = 1.0), group 6 elements 3-6. **b** USAF target in immersion (n = 1.4), group 7 elements 1-5.

As typical for CFB-based endoscopes, images acquired with our device suffer from artifacts due to the CFB’s pixelation, impairing the visual recognition. We perform Gaussian smoothing and median filtering to reduce the negative effect of the pixelation, aiming to improve the perceived feature recognition.

We study the effect of filtering procedures on the images of the USAF resolution target in Fig. 6**c** from the main manuscript (Fig. S5). We subject all images to dark-subtraction. The images without further filtering (left column) show characteristic pixelation effects. In the images to the right, we apply a median filter with a kernel size of 10 pixels (4.8 µm), combined with a Gaussian smoothing-filter with increasing standard deviation σ of the Gauss kernel.

The additional median and Gaussian filters increasingly remove the CFB pixelation pattern, improving the perceived visual clarity with increasing σ. We found the best perceived visual clarity with σ close to the average inter-core cladding-width (pitch = 3.2 µm, core-diameter = 2 µm [3] → inter-core cladding-width = 1.2 µm). We therefore used these images in the main manuscript. Increasing σ beyond this value blurs the image without further benefit, and hence in our opinion should be avoided.

Supplementary information for: Marco Wende, Jule Grunewald, Ada Bachmann, Fabian Wilde, Michael Heymann, Alois M. Herkommer, Valese Aslani, and Andrea Toulouse. “Illumination and microscopy combined in a single fibre bundle by 3D-printed micro-optics”. Light: Advanced Manufacturing

5. Illumination efficiency and light-coupling losses

To estimate the illumination efficiency and assess possible sources of loss in our system, we measure the available LED illumination power with a power meter (PM160, Thorlabs, Newton, New Jersey, USA). Fig. S6 shows the measured illumination power and losses. Initially, ~ 350 µW illumination light from the LED are directed towards the CFB. We measure ~ 275 µW light transmitted beside the CFB, and ~ 6 µW reflected from the CFB back-end – both constituting losses. At the CFB front-end, we measure ~ 0.3 µW illumination light at the sample plane.

The ring-DOE covers 33 % of the CFB, and hence only this area is available for illumination coupling - light incident at the residual 67 % of the facet is lost. The following issues contribute to loss of light too, but are difficult to quantify at the full-endoscope system level:

- The CFB-pixelation reduces the area available for light transportation, because the lossy cladding rejects incident light
- Out-coupling at the CFB front-end and waveguide-losses in the 3D-printed structure

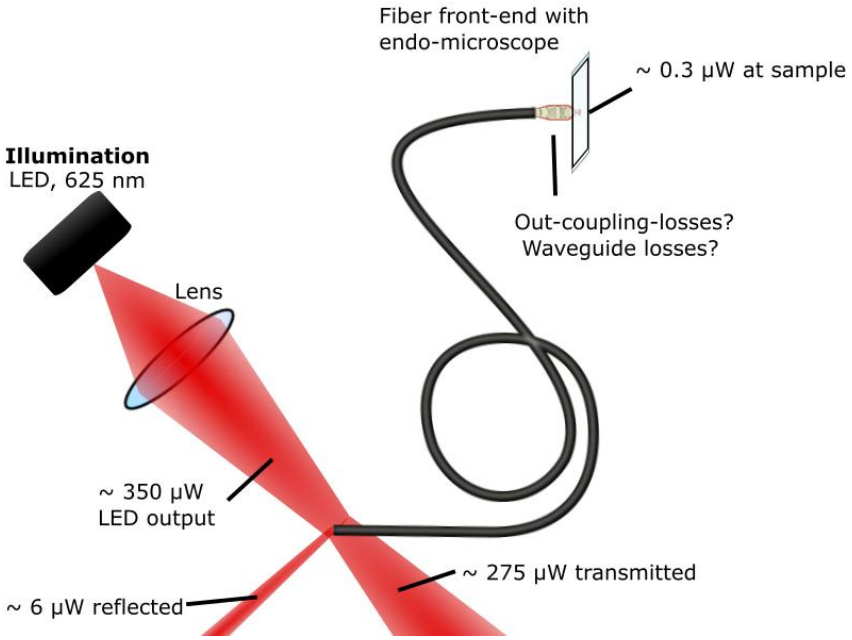

Fig. S6: Measurements of illumination power and losses.

The following engineering approaches and trade-offs promise to improve the illumination at the sample plane, allowing to increase the endoscope’s frame rate in future applications:

- brighter LEDs are commercially available to increase the incident illumination light
- illumination is relayed to the CFB with a $\emptyset_{Spot} > \emptyset_{CFB}$. While this simplifies alignment significantly, it causes high loss (> 75 %). A relay lens with a smaller focal length would create a tighter focus and raises alignment requirements, but allows to increase the illumination efficiency.
- increasing the area covered by the ring-DOE reduces the area available for imaging, but raises the illumination coupling efficiency
- the CFB-pixelation reduces the CFB-area effectively available for illumination coupling. Combining the ring-DOE with a microlens-array, tailored to the specific CFB, could improve the illumination yield by a factor of ~1.75 [5].

Supplementary information for: Marco Wende, Jule Grunewald, Ada Bachmann, Fabian Wilde, Michael Heymann, Alois M. Herkommer, Valese Aslani, and Andrea Toulouse. “Illumination and microscopy combined in a single fibre bundle by 3D-printed micro-optics”. Light: Advanced Manufacturing

References

[1] Hughes, M. R. Real-timing processing of fiber bundle endomicroscopy images in python using pyfibrebundle. *Applied optics* **62**, 9041–9050 (2023)

[2] Gálvez, D. et al. Resolution cascade: simulated MTF of a coherent fiber bundle-based microendoscopic system. *Applied Optics* **65**, 637–645 (2026).

[3] Chen, X., Reichenbach, K. L. & Xu, C. Experimental and theoretical analysis of core-to-core coupling on fiber bundle imaging. *Optics express* **16**, 21598–21607 (2008).

[4] Born, M. & Wolf, E. Principles of optics: Electromagnetic theory of propagation, interference and diffraction of light (Elsevier, 2013).

[5] Roy, S. et al. Tailored 3D-printed microlens arrays for increased illumination efficiency in imaging fiber bundles. In Optical Fibers and Sensors for Medical Diagnostics, Treatment, and Environmental Applications XXVI, Vol. 13842, 229–236 (SPIE, 2026).